IEEE Access
Multidisciplinary | Rapid Review | Open Access Journal

Date of publication xxxx 00, 0000, date of current version xxxx 00, 0000.

Digital Object Identifier 10.1109/ACCESS.2017.DOI

Finite-Time Observer Based Guidance and Control of Underactuated Surface Vehicles with Unknown Sideslip Angles and Disturbances

NING WANG[1], (Senior Member, IEEE), ZHUO SUN[1], JIANCHUAN YIN[2], (Member, IEEE), SHUN-FENG SU[3], (Fellow, IEEE), and SANJAY SHARMA[4], (Senior Member, IEEE).

[1]Center for Intelligent Marine Vehicles, School of Marine Electrical Engineering, Dalian Maritime University, Dalian 116026, P. R. China.
[2]Center for Intelligent Marine Vehicles, Navigation College, Dalian Maritime University, Dalian 116026, P. R. China.
[3]Department of Electrical Engineering, National Taiwan University of Science and Technology, Taiwan, P. R. China.
[4] School of Engineering, Plymouth University, Plymouth, Devon PL4 8AA, UK.

Corresponding author: N. Wang (n.wang.dmu.cn@gmail.com)

This work is supported by the National Natural Science Foundation of P. R. China (under Grants 51009017 and 51379002), Applied Basic Research Funds from Ministry of Transport of P. R. China (under Grant 2012-329-225-060), China Postdoctoral Science Foundation (under Grant 2012M520629), the Fund for Dalian Distinguished Young Scholars (under Grant 2016RJ10), the Innovation Support Plan for Dalian Highlevel Talents (under Grant 2015R065), and the Fundamental Research Funds for the Central Universities (under Grant 3132016314).

ABSTRACT Suffering from complex sideslip angles, path following control of an underactuated surface vehicle (USV) becomes significantly challenging and remains unresolved. In this paper, a finite-time observer based guidance and control (FOGC) scheme for path following of an USV with time-varying and large sideslip angles and unknown external disturbances is proposed. The salient features of the proposed FOGC scheme are as follows: (1) Time-varying large sideslip angle is exactly estimated by a finite-time sideslip observer (FSO), and thereby contributing to the sideslip-tangent line-of-sight (SLOS) guidance law which significantly enhances the robustness of the guidance system to unknown sideslip angles which are significantly large and time-varying; (2) A finite-time disturbance observer (FDO) is devised to exactly observe unknown external disturbances, and thereby implementing FDO based surge and heading robust tracking controllers which possess remarkable tracking accuracy and precise disturbance rejection, simultaneously. (3) By virtue of cascade analysis and Lyapunov approach, global asymptotic stability of the integrated guidance-control system is rigorously ensured. Simulation studies and comparisons are conducted to demonstrate the effectiveness and superiority of the proposed FOGC scheme.

INDEX TERMS Finite-time sideslip observer, sideslip-tangent line-of-sight guidance, integrated guidance and control, underactuated surface vehicles, path following.

I. INTRODUCTION

Over the past decades, the development of underactuated surface vehicles (USVs) has greatly contributed to marine military and commerce due to the ability to autonomously execute various high-risk maritime missions which may include water quality detection, long-duration oceanographic sampling, undersea mines, mine clearance, pipeline inspection, *etc*. [1]–[4], and thereby dramatically reducing the risk of casualties and misuse. To be specific, the underactuated characteristics of an USV feature various advantages in reducing sensor costs and weights. However, much more powerful navigation, guidance and control techniques [5]–[8] are desirably required to ensure promising performance with underactuated constraints. In this context, motion control of an USV has been being a hot research area and has attracted numerous researchers. Path following problem represents a pivotal control scenario where the USV is expected to autonomously follow a predefined path which may exclude time constraints. It should be noted that path-tracking problems arise from following a time-constrained path with a desired surge speed [9]. As a consequence, high-accuracy path following control technology becomes crucial in executing various crucial missions, and thereby determining the technical level and comprehensive performance of the USV.

This article has been accepted for publication in a future issue of this journal, but has not been fully edited. Content may change prior to final publication. Citation information: DOI 10.1109/ACCESS.2018.2797084, IEEE Access

Path following control scheme of an USV usually consists of two modules, i.e., guidance and control subsystems [10]–[12]. The former part attempts to generate reference signals by addressing path information together with environments for the latter one. Accordingly, the control system produces the actual signals to track the reference signals governed by the guidance system. In this context, the guidance system acts a decisive role in the entire path-following system. Note that the line-of-sight (LOS) guidance method provides a promising algorithm for path following of an USV. At the early stage, an LOS projection algorithm in [11] was deployed to follow a segmented path which is connected by successive way-points, whereby the switching mechanism facilitated target point selection and path switching. The proportional line-of-sight (PLOS) guidance law for straight-line path following was addressed by Pettersen [13] and Fossen [14], respectively, whereby the guided heading angle was derived from the arctangent value of the cross-track error and the lookahead distance. In previous works, guidance laws are susceptible to environmental disturbances due to ocean wind, waves and currents, and sideslip angles are actually assumed to be zero. Since the sideslip angle may amplify path following errors and even would destroy system stability, compensations for sideslip angles are required. In [15], [16], integral actions were nested into the PLOS guidance law thereby leading to the integral line-of-sight (ILOS) guidance law, and were expected to counteract influences of environmental disturbances. By encapsulating the sideslip angle into the course angle, the ILOS guidance with integral of cross-track errors was developed in [17]. In addition, an LOS guidance law using adaptive sideslip angle compensation (i.e., ALOS) was proposed in [18], whereby the sideslip angle was dominated by an adaptive term. In fact, the foregoing ALOS method can be seen as a special case of ILOS guidance with slow time-varying or constant sideslip angles. Taking time-varying sideslip angles into account, an observer based guidance law was proposed by employing an adaptive sideslip observer in [19] and a linear extended state sideslip observer in [20], respectively. However, the sideslip angle has to be approximated by a small-angle linearization. Nevertheless, the observation errors can only ensure asymptotic convergence, which does not achieve fast and exact sideslip angle compensation. It should also be pointed out that the aforementioned guidance laws in [13]–[18] have a strict restriction that the cross-track error is required to be smaller than the smallest radius of curvature present on the predefined path, since the projection point of the USV onto the path is selected as the "target point" to be followed.

Within a entire path following scheme, the control subsystem is taken as an execution module, whereby various control techniques can be utilized. In [21], linear model predictive control (MPC) was used for the nonlinear ship maneuvering control where the developed ship model can be linearized to obtain the time-varying linear predictive model, thereby simplifying the optimization task. A global finite-time controller based on sliding mode control (SMC) method was proposed in [22], whereby the surge and heading tracking errors converge to zero in a finite time. In addition, a singular perturbation control strategy for path following was proposed in [23]. However, the foregoing controllers cannot address external disturbances. Using the backstepping technique, nonlinear tracking controllers can be derived in [24], [25], whereby the upper bounds of external disturbances were identified by an adaptive term. In [26], robust adaptive technique was integrated in the decentralized chattering free sliding control design in order to handle unknown bounded uncertainties. In [27], [28], radial basis function neural networks were used to approximate the nonlinear uncertainties including unmodeled dynamics and unknown disturbances. Recently, a disturbance observer based MPC approach was proposed in [29] where disturbances can be asymptotically rejected. Increasingly, fuzzy/neural approaches [30]–[35] have also been successfully employed to approximate uncertainties and/or unmodeled dynamics within the guidance and control scheme of underactuated marine vehicles. Moreover, fuzzy/neural approximators can be made self-constructive by virtue of growing and pruning mechanisms [36], [37], as well as adaptive universe [38]. It should be noted that the foregoing self-constructive fuzzy/neural approaches achieve remarkable superiority in terms of both online approximation and tracking accuracy. Besides, the active disturbance rejection control (ADRC) [39] and nonlinear disturbance observer (NDO) [40] approaches have also be utilized to estimate unknown disturbances pertaining to an USV. However, observation errors are usually globally uniformly ultimately bounded rather than accurate estimate. Lately, by virtue of adding a power integrator [41] and nonsingular terminal sliding mode [42], Wang et al. [8], [43], [44] created a fast and accurate trajectory tracking control framework for fully-actuated marine vehicles, whereby uncertainties and/or disturbances can be exactly observed and the entire tracking errors can converge to zero within a finite time rather than asymptotic/exponential convergence. Interestingly, in [45], a second-order sliding mode observer and adaptive fuzzy approximators have been deployed to exclusively address time-varying sideslip angles and unknown dynamics, respectively. Unfortunately, unknown disturbances cannot be tackled yet. To the best of our knowledge, counterpart solutions to an USV suffering from time-varying sideslip angle with a large range together with complex unknowns including uncertainties and/or disturbances are largely open.

Motivated by above observations, a finite-time observer based guidance and control (FOGC) scheme is proposed to deal with both time-varying large sideslip angles and external disturbances which are unknown simultaneously. As a consequence, curved path following of an USV can be achieved with high accuracy. The finite-time sideslip observer (FSO) is deployed to exactly identify unknown sideslip angle which is allowed to be large and time-varying. With accurate sideslip observation, the FSO-based sideslip-tangent LOS (SLOS) guidance law is further developed, whereby accurate sideslip angle compensation and enhanced

This article has been accepted for publication in a future issue of this journal, but has not been fully edited. Content may change prior to final publication. Citation information: DOI 10.1109/ACCESS.2018.2797084, IEEE Access

robustness of the guidance system to unknown sideslip angle can be simultaneously achieved. Moreover, the finite-time disturbance observer (FDO) is created to exactly observe unknown external disturbances. In this context, the FDO-based robust tracking controllers for surge and heading dynamics can ensure accurate tracking of the reference signals produced by the proposed SLOS guidance law. Eventually, using cascade analysis, the entire guidance-control system is guaranteed to be globally asymptotically stable.

The rest of this paper is organized as follows. Section II formulates preliminaries and path following problem of an USV under complex sideslip angles and disturbances. Section III derives path following error dynamics. The finite-time sideslip observer and the SLOS guidance law are developed in Sections IV and V, respectively. The finite-time disturbance observer is developed in Section VI. Surge and heading tracking controllers and stability analysis of the entire guidance-control closed-loop system are addressed in Sections VII and VIII, respectively. Simulation studies and comparisons are conducted in Section IX. Section X concludes this paper.

II. PRELIMINARIES AND PROBLEM FORMULATION

A. PRELIMINARIES

Lemma 1: ([46]) Consider the following cascade system:

$$\begin{aligned}\dot{x}_c &= f(x_c, \omega_c)\\ \dot{\omega}_c &= s(\omega_c)\end{aligned} \tag{1}$$

where $x_c \in \mathrm{R}^n$, $\omega_c \in \mathrm{R}^m$, $f : \mathrm{R}^n \times \mathrm{R}^m \to \mathrm{R}^n$ and $s : \mathrm{R}^m \to \mathrm{R}^m$ are both C^1 vector fields. In addition, $f(0,0) = 0$, $s(0) = 0$, so that $(x_c, \omega_c) = (0,0)$ is an equilibrium of the cascade system (1).

Suppose that $x_c = 0$ is a globally asymptotically stable equilibrium of the subsystem

$$\dot{x}_c = f(x_c, 0) \tag{2}$$

$\omega_c = 0$ is a globally asymptotically stable equilibrium of the subsystem

$$\dot{\omega}_c = s(\omega_c) \tag{3}$$

and that all the trajectories $(x_c(t), \omega_c(t))$ of (1) are bounded for $t > 0$. Then $(x_c, \omega_c) = (0,0)$ is a globally asymptotically stable equilibrium of the cascade system (1).

Lemma 2: ([47]) The following system:

$$\begin{aligned}\dot{\sigma}_0 =& -\lambda_0 L^{1/(n+1)} |\sigma_0|^{n/n+1} \mathrm{sgn}(\sigma_0) + \sigma_1\\ \dot{\sigma}_1 =& -\lambda_1 L^{1/n} |\sigma_1 - \dot{\sigma}_0|^{n/n+1} \mathrm{sgn}(\sigma_1 - \dot{\sigma}_0) + \sigma_2\\ &\vdots\\ \dot{\sigma}_{n-1} =& -\lambda_{n-1} L^{1/2} |\sigma_{n-1} - \dot{\sigma}_{n-2}|^{1/2} \mathrm{sgn}(\sigma_{n-1} - \dot{\sigma}_{n-2})\\ &+ \sigma_n\\ \dot{\sigma}_n \in& -\lambda_n L \mathrm{sgn}(\sigma_n - \dot{\sigma}_{n-1}) + [-L, L]\end{aligned} \tag{4}$$

where $L > 0$ and $\lambda_i > 0$, $i = 0, 1, \cdots, n$ are appropriate constants, is finite-time stable.

B. USV MODEL

The USV kinematics on the horizontal plane can be described as follows [48]:

$$\begin{aligned}\dot{x} &= u\cos\psi - v\sin\psi\\ \dot{y} &= u\sin\psi + v\cos\psi\\ \dot{\psi} &= r\end{aligned} \tag{5}$$

where (x, y, ψ) are position coordinates and orientation of the USV with respect to the earth-fixed frame, (u, v, r) are surge, sway and yaw velocities within the body-fixed frame.

Usually, a generic assumption is required.

Assumption 1: ([20]) The following settings hold:

1) The center of gravity coincides with the center of buoyancy;
2) The mass distribution of the USV is homogeneous and the vessel is rigid body;
3) The shape structure of the USV is starboard symmetric;
4) The heave, pitch, and roll motions are neglected in path following on the horizontal plane.

The dynamics of an USV are modeled by

$$\begin{aligned}m_{11}\dot{u} &= m_{22}vr - d_{11}u + \tau_u + \tau_{\delta_u}\\ m_{22}\dot{v} &= -m_{11}ur - d_{22}v + \tau_{\delta_v}\\ m_{33}\dot{r} &= -(m_{22} - m_{11})uv - d_{33}r + \tau_r + \tau_{\delta_r}\end{aligned} \tag{6}$$

where $d_{11}, d_{22}, d_{33}, m_{11}, m_{22}, m_{33}$ denote the hydrodynamic damping and ship inertia including added mass in surge, sway and yaw. The available controls are only the surge force τ_u and the yaw moment τ_r, so the path following control of USV is an underactuated control problem [49]. $\boldsymbol{\tau}_\delta = [\tau_{\delta_u}, \tau_{\delta_v}, \tau_{\delta_r}]^T$ are the unknown external disturbances in surge, sway, yaw directions, which are estimated accurately by the constructed FDO. In what follows, surge and heading robust tracking controllers based on the FDO are synthesized to render the actual surge velocity and heading angle track accurately the guided values generated by the guidance system in presence of unknown external disturbances, and the corresponding tracking errors can asymptotically converge to the origin.

III. PATH FOLLOWING ERROR DYNAMICS

As shown in Fig. 1, a geometric curved path is parameterized by a time-dependent path variable ϖ. A path-tangent reference coordinate frame is defined at the point $(x_p(\varpi), y_p(\varpi))$, and is rotated with an angle ϕ_p relative to the earth-fixed coordinate frame given by

$$\phi_p = \mathrm{atan2}\left(y_p'(\varpi), x_p'(\varpi)\right) \tag{7}$$

where $x_p'(\varpi) = \partial x_p/\partial\varpi$, $y_p'(\varpi) = \partial y_p/\partial\varpi$, and the function $\mathrm{atan2}(y, x)$ returns the angle between the positive x-axis of a plane and the point given by the coordinates (x, y) on it.

For an USV located at the point (x, y), the corresponding path-following errors between (x, y) and $(x_p(\varpi), y_p(\varpi))$

This article has been accepted for publication in a future issue of this journal, but has not been fully edited. Content may change prior to final publication. Citation information: DOI 10.1109/ACCESS.2018.2797084, IEEE Access

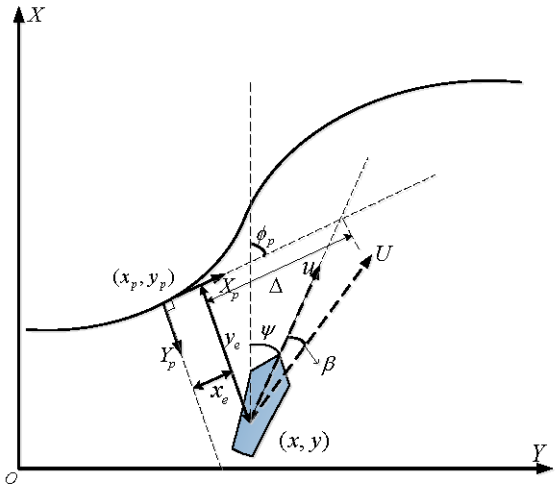

FIGURE 1. Path following control geometry of an USV.

expressed in the path-tangential coordinate frame are as follows:

$$\begin{bmatrix} x_e \\ y_e \end{bmatrix} = \begin{bmatrix} \cos\phi_p & -\sin\phi_p \\ \sin\phi_p & \cos\phi_p \end{bmatrix}^T \begin{bmatrix} x - x_p \\ y - y_p \end{bmatrix} \tag{8}$$

where y_e and x_e are cross- and along-track errors, respectively.

Similar to [17], taking time derivatives along (5), path-following error dynamics can be written as follows:

$$\begin{aligned}
\dot{x}_e =& (u\cos\psi - v\sin\psi)\cos\phi_p \\
&+ (u\sin\psi + v\cos\psi)\sin\phi_p \\
&+ \underbrace{[-\sin\phi_p(x - x_p) + \cos\phi_p(y - y_p)]}_{\text{cross-track error } \ y_e}\dot{\phi}_p \\
&- (u_{\text{tar}}\sin^2\phi_p + u_{\text{tar}}\cos^2\phi_p) \\
=& u\cos(\psi - \phi_p) - v\sin(\psi - \phi_p) + \dot{\phi}_p y_e - u_{\text{tar}} \\
\dot{y}_e =& -(u\cos\psi - v\sin\psi)\sin\phi_p \\
&+ (u\sin\psi + v\cos\psi)\cos\phi_p \\
&+ \underbrace{[\cos\phi_p(x - x_p) + \sin\phi_p(y - y_p)]}_{\text{along-track error } \ x_e}\dot{\phi}_p \\
&+ (u_{\text{tar}}\cos\phi_p\sin\phi_p - u_{\text{tar}}\sin\phi_p\cos\phi_p) \\
=& u\sin(\psi - \phi_p) + v\cos(\psi - \phi_p) - \dot{\phi}_p x_e
\end{aligned} \tag{9}$$

where u_{tar} is the virtual target speed along the curved path, and is governed by

$$u_{\text{tar}} = \dot{\varpi}\sqrt{x_p'^2(\varpi) + y_p'^2(\varpi)} \tag{10}$$

In addition, the sideslip angle is defined as follows:

$$\beta = \text{atan2}(v, u) \tag{11}$$

Hence, the course angle φ can be derived

$$\varphi = \psi + \beta \tag{12}$$

Together with (11), path-following error dynamics (9) can be reformulated by

$$\begin{aligned}
\dot{x}_e &= u\cos(\psi - \phi_p) - u\sin(\psi - \phi_p)\tan\beta + \dot{\phi}_p y_e - u_{\text{tar}} \\
\dot{y}_e &= u\sin(\psi - \phi_p) + u\cos(\psi - \phi_p)\tan\beta - \dot{\phi}_p x_e
\end{aligned} \tag{13}$$

Remark 1: Different from previous works [15]–[20], a time-varying large sideslip angle β does not need small-angle approximation, i.e., $\sin\beta \simeq \beta$ and $\cos\beta \simeq 1$.

IV. FINITE-TIME SIDESLIP OBSERVER

In order to exactly identify thetime-varying large sideslip angle β, similar to [45], a finite-time sideslip observer (FSO) is developed in this section.

From (13), we have

$$\dot{y}_e = g(u, \psi, \phi_p, \beta) + u\sin(\psi - \phi_p) - \dot{\phi}_p x_e \tag{14}$$

where

$$g(u, \psi, \phi_p, \beta) = u\cos(\psi - \phi_p)\tan\beta \tag{15}$$

It should be noted that the nonlinearity $g(\cdot)$ is C^1 differentiable.

Proposition 1: There exists an appropriate constant $G > 0$ such that $|\dot{g}| \leq G < \infty$.

Proof 1: Using (6), we have

$$\begin{aligned}
\dot{g} &= \dot{v}\cos(\psi - \phi_p) - v\sin(\psi - \phi_p)(\dot{\psi} - \dot{\phi}_p) \\
&= \frac{\cos(\psi - \phi_p)}{m_{22}}(-m_{11}ur - d_{22}v) \\
&\quad - v\sin(\psi - \phi_p)(r - \dot{\phi}_p)
\end{aligned} \tag{16}$$

For an USV, u, v and r are bounded. In addition, $\dot{\phi}_p$ is also bounded. It follows that there exists a finite value $G > 0$ satisfying $|\dot{g}| \leq G < \infty$.

This concludes the proof.

Theorem 1: Using the FSO as follows:

$$\begin{aligned}
\dot{\hat{y}}_e &= \delta_0 + u\sin(\psi - \phi_p) - \dot{\phi}_p x_e \\
\delta_0 &= -\lambda_1 L_\beta^{1/2}\text{sig}^{1/2}(\hat{y}_e - y_e) + \hat{g} \\
\dot{\hat{g}} &= -\lambda_2 L_\beta \text{sgn}(\hat{g} - \delta_0)
\end{aligned} \tag{17}$$

where $\lambda_i > 0$, $i = 1, 2$, $L_\beta > 0$ and $\text{sig}^\alpha(x) = |x|^\alpha\text{sgn}(x)$, the term g in (13) can be exactly identified within a finite time.

Proof 2: Define observation errors as follows:

$$\begin{aligned}
e_1 &= \hat{y}_e - y_e \\
e_2 &= \hat{g} - g
\end{aligned} \tag{18}$$

This article has been accepted for publication in a future issue of this journal, but has not been fully edited. Content may change prior to final publication. Citation information: DOI 10.1109/ACCESS.2018.2797084, IEEE Access

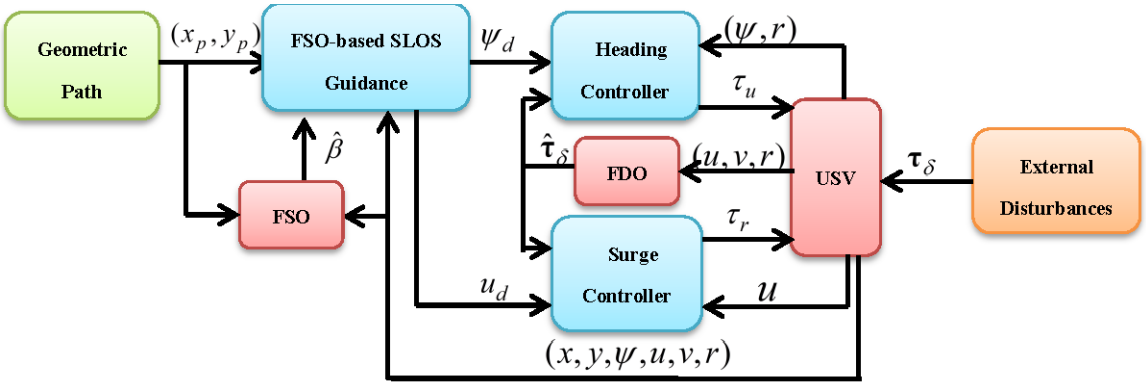

FIGURE 2. The block diagram of the FOGC scheme.

we have

$$\begin{aligned}\dot{e}_1 =& \dot{\hat{y}}_e - \dot{y}_e \\ =& -\lambda_1 L_\beta^{1/2} \mathrm{sig}^{1/2}(\hat{y}_e - y_e) + \hat{g} + u\sin(\psi - \phi_p) \\ & - \dot{\phi}_p x_e - \dot{y}_e \\ =& -\lambda_1 L_\beta^{1/2} \mathrm{sig}^{1/2}(\hat{y}_e - y_e) + \hat{g} - g \\ =& -\lambda_1 L_\beta^{1/2} \mathrm{sig}^{1/2}(e_1) + e_2 \\ \dot{e}_2 =& \dot{\hat{g}} - \dot{g} \\ \in& -\lambda_2 L_\beta \mathrm{sgn}(e_2 - \dot{e}_1) + [-G, G] \end{aligned} \tag{19}$$

By Lemma 2, we immediately have observation errors e_1 and e_2 converge to zero within a short time, i.e., there exists a finite time $0 < T_\beta < \infty$ such that

$$\hat{y}_e(t) \equiv y_e(t), \quad \hat{g}(t) \equiv g(t), \quad \forall t \geq T_\beta \tag{20}$$

This concludes the proof.

Remark 2: The FSO preserves faster convergence rate and stronger disturbance rejection ability, simultaneously. In theory, the FSO observation errors can exactly converge to zero within a short time, and thereby contributing to zero-error accuracy. However, traditional asymptotic approaches can only achieve infinite-time convergence.

V. FSO-BASED SIDESLIP-TANGENT LOS GUIDANCE

As shown in Fig. 2, a sideslip-tangent line-of-sight (SLOS) guidance scheme based on the FSO is proposed by combining with heading and "virtual target" guidance laws.

The heading guidance is determined by

$$\psi_d = \phi_p - \arctan\left(\tan\hat{\beta} + \frac{y_e}{\Delta}\right) \tag{21}$$

where $\Delta > 0$ is the lookahead distance, and the sideslip angle estimate $\hat{\beta}$ is governed by

$$\hat{\beta} = \arctan\frac{\hat{g}}{u\cos(\psi - \phi_p)} \tag{22}$$

here, $\hat{g}$ is given by (17).

The "virtual target" guidance is determined by

$$u_{\mathrm{tar}} = k_1 x_e + U\cos\left(\psi - \phi_p + \hat{\beta}\right) \tag{23}$$

where $k_1 > 0$, and $U = \sqrt{u^2 + v^2}$ is the USV course speed.

Remark 3: From (21), we have

$$\begin{aligned}\psi - \phi_p \simeq& \psi_d - \phi_p \\ =& -\arctan\left(\tan\hat{\beta} + \frac{y_e}{\Delta}\right) \in (-\pi/2, \pi/2) \end{aligned} \tag{24}$$

In addition, by increasing Δ, there exists a positive value $\varsigma > 0$ such that $\cos(\psi - \phi_p) > \varsigma$. Eventually, the singularity can be avoided if the surge velocity is uniformly positive.

Remark 4: Unlike the approach in [9] whereby a desired surge speed is required to be determined, the velocity guidance law in (23) aims to directly guide the virtual ship along the path to be tracked by an USV. In addition, the velocity u_{tar} is actually an FSO-based surge guidance for the virtual ship, and can exactly estimate unknown sideslip angles which are allowed to be time-varying and large.

Theorem 2: Consider the path following system (13) together with the guidance scheme (17), (21)–(23), both along- and cross-track path-following errors can be made asymptotically stable.

Proof 3: Using the following facts:

$$\begin{aligned}\sin(\psi - \phi_p) &= -\frac{y_e + \Delta\tan\hat{\beta}}{\sqrt{\Delta^2 + (y_e + \Delta\tan\hat{\beta})^2}} \\ \cos(\psi - \phi_p) &= -\frac{\Delta}{\sqrt{\Delta^2 + (y_e + \Delta\tan\hat{\beta})^2}}\end{aligned}$$

and substituting (21)–(23) into (13) yields

$$\begin{aligned}\dot{x}_e =& -k_1 x_e + \dot{\phi}_p y_e - u\sin(\psi - \phi_p)(\tan\beta - \tan\hat{\beta}) \\ \dot{y}_e =& -\frac{u}{\sqrt{\Delta^2 + (y_e + \Delta\tan\hat{\beta})^2}} y_e - \dot{\phi}_p x_e \\ & + \frac{\Delta u}{\sqrt{\Delta^2 + (y_e + \Delta\tan\hat{\beta})^2}}(\tan\beta - \tan\hat{\beta}) \end{aligned} \tag{25}$$

This article has been accepted for publication in a future issue of this journal, but has not been fully edited. Content may change prior to final publication. Citation information: DOI 10.1109/ACCESS.2018.2797084, IEEE Access

From Theorem 1, one can derive $\tan\beta - \tan\hat{\beta} \equiv 0, \forall t \geq T_{\text{obs}}$. It follows that for any $t \geq T_\beta$

$$\begin{aligned}\dot{x}_e &= -k_1 x_e + \dot{\phi}_p y_e \\ \dot{y}_e &= -\frac{u}{\sqrt{\Delta^2 + (y_e + \Delta\tan\beta)^2}} y_e - \dot{\phi}_p x_e\end{aligned} \tag{26}$$

Consider the Lyapunov function as follows:

$$V_1 = \frac{1}{2}(x_e^2 + y_e^2) \tag{27}$$

Differentiating V_1 along (26) yields

$$\dot{V}_1 = -k_1 x_e^2 - \frac{u}{\sqrt{\Delta^2 + (y_e + \Delta\tan\beta)^2}} y_e^2 \tag{28}$$

where $k_1 > 0$, and $u_{\max} \geq u \geq u_{\min} > 0$.

It implies that V_1 is bounded, i.e., $|x_e| \leq \bar{x}_e$ and $|y_e| \leq \bar{y}_e$ are bounded. From (28), we further have

$$\begin{aligned}\dot{V}_1 &= -k_1 x_e^2 - \frac{u^2}{\sqrt{\Delta^2 u^2 + (u y_e + \Delta v)^2}} y_e^2 \\ &\leq -k_1 x_e^2 - k_2 y_e^2 \\ &\leq -k V_1\end{aligned} \tag{29}$$

where

$$\begin{aligned}k &= 2\min\{k_1, k_2\} \\ k_2 &= \frac{u_{\min}^2}{\sqrt{\Delta^2 u_{\max}^2 + (u_{\max}\bar{y}_e + \Delta v_{\max})^2}}\end{aligned}$$

with $v_{\max} \geq v \geq v_{\min} > 0$.

This concludes the proof.

VI. FINITE-TIME DISTURBANCE OBSERVER

The dynamic model (6) can be formulated as follows:

$$\boldsymbol{M}\dot{\boldsymbol{\nu}} = \boldsymbol{f}(\boldsymbol{\nu}) + \boldsymbol{\tau} + \boldsymbol{\tau}_\delta \tag{30}$$

where $\boldsymbol{\nu} = [u, v, r]^T$, $\boldsymbol{M} = \text{diag}(m_{11}, m_{22}, m_{33})$, $\boldsymbol{\tau} = [\tau_u, 0, \tau_r]^T$,$\boldsymbol{\tau}_\delta = [\tau_{\delta_u}, \tau_{\delta_v}, \tau_{\delta_r}]^T$, $\boldsymbol{f}(\boldsymbol{\nu}) = [f_u, f_v, f_r]^T$ that are theoretically formulated as follows:

$$\begin{aligned}f_u &= m_{22} v r - d_{11} u \\ f_v &= -m_{11} u r - d_{22} v \\ f_r &= -(m_{22} - m_{11}) u v - d_{33} r\end{aligned} \tag{31}$$

Assumption 2: The external disturbances $\boldsymbol{\tau}_\delta$ satisfies

$$\|\dot{\boldsymbol{\tau}}_\delta\| \leq D \tag{32}$$

for a bounded constant $D < \infty$.

Remark 5: When the USV is disturbed by unknown external disturbances, it is usually considered that the disturbances are superimposed by the low frequency period signals [8], so the assumption is reasonable in practice.

Among that, $\boldsymbol{\tau}_\delta$ estimated by the following finite-time disturbance observer (FDO):

$$\begin{aligned}\boldsymbol{M}\dot{\hat{\boldsymbol{\nu}}} &= \boldsymbol{\zeta} + \boldsymbol{f}(\boldsymbol{\nu}) + \boldsymbol{\tau} \\ \boldsymbol{\zeta} &= -\lambda_3 \boldsymbol{L}_\delta^{1/2} \text{sig}^{1/2}(\boldsymbol{M}\hat{\boldsymbol{\nu}} - \boldsymbol{M}\boldsymbol{\nu}) + \hat{\boldsymbol{\tau}}_\delta \\ \dot{\hat{\boldsymbol{\tau}}}_\delta &= -\lambda_4 \boldsymbol{L}_\delta \text{sgn}(\hat{\boldsymbol{\tau}}_\delta - \boldsymbol{\zeta})\end{aligned} \tag{33}$$

where $\boldsymbol{\zeta} = [\zeta_u, \zeta_v, \zeta_r]^T$, $\boldsymbol{L}_\delta = \text{diag}(l_u, l_v, l_r)$, $l_k > 0$, $k = u, v, r$, $\lambda_j > 0, j = 3, 4$, $\hat{\boldsymbol{\tau}}_\delta = [\hat{\tau}_{\delta_u}, \hat{\tau}_{\delta_v}, \hat{\tau}_{\delta_r}]^T$ is the estimate of the external disturbances.

Theorem 3: Using the constructed FDO (33), unknown disturbances $\boldsymbol{\tau}_\delta$ can be exactly identified within a short time.

Proof 4: Define

$$\begin{aligned}\boldsymbol{e}_3 &= \boldsymbol{M}\hat{\boldsymbol{\nu}} - \boldsymbol{M}\boldsymbol{\nu} \\ \boldsymbol{e}_4 &= \hat{\boldsymbol{\tau}}_\delta - \boldsymbol{\tau}_\delta\end{aligned} \tag{34}$$

we have

$$\begin{aligned}\dot{\boldsymbol{e}}_3 =& \boldsymbol{M}\dot{\hat{\boldsymbol{\nu}}} - \boldsymbol{M}\dot{\boldsymbol{\nu}} \\ =& -\lambda_3 \boldsymbol{L}_{\boldsymbol{\delta}}^{1/2} \text{sig}^{1/2}(\boldsymbol{M}\hat{\boldsymbol{\nu}} - \boldsymbol{M}\boldsymbol{\nu}) + \hat{\boldsymbol{\tau}}_\delta \\ &+ \boldsymbol{f}(\boldsymbol{\nu}) + \boldsymbol{\tau} - \boldsymbol{M}\dot{\boldsymbol{\nu}} \\ =& -\lambda_3 \boldsymbol{L}_{\boldsymbol{\delta}}^{1/2} \text{sig}^{1/2}(\boldsymbol{e}_3) + \boldsymbol{e}_4 \\ \dot{\boldsymbol{e}}_4 =& \dot{\hat{\boldsymbol{\tau}}}_\delta - \dot{\boldsymbol{\tau}}_\delta \\ =& -\lambda_4 \boldsymbol{L}_{\boldsymbol{\delta}} \text{sgn}(\hat{\boldsymbol{\tau}}_\delta - \boldsymbol{\zeta}) - \dot{\boldsymbol{\tau}}_\delta \\ \in& -\lambda_4 \boldsymbol{L}_{\boldsymbol{\delta}} \text{sgn}(\boldsymbol{e}_4 - \dot{\boldsymbol{e}}_3) + [-D, D]\end{aligned} \tag{35}$$

Using Lemma 2, observation errors $\boldsymbol{e}_3$ and $\boldsymbol{e}_4$ can converge to zero in a finite time, i.e., there exists a finite time $0 < T_\delta < \infty$ such that

$$\hat{\boldsymbol{\nu}}(t) \equiv \boldsymbol{\nu}(t), \;\; \hat{\boldsymbol{\tau}}_\delta(t) \equiv \boldsymbol{\tau}_\delta(t), \;\; \forall t \geq T_\delta \tag{36}$$

This concludes the proof.

VII. SURGE AND HEADING CONTROL

A. SURGE CONTROL

Theorem 4: Consider surge dynamics in (6), and an FDO-based robust surge tracking control law as follows:

$$\tau_u = -m_{22} v r + d_{11} u - \hat{\tau}_{\delta_u} - m_{11}(k_u u_e - \dot{u}_d) \tag{37}$$

where $k_u > 0$, u_d is the desire surge velocity, $u_e = u - u_d$ is the surge tracking error, and $\hat{\tau}_{\delta_u}$ is the estimate of external disturbances in surge obtained in (33). Then, the desired surge speed u_d can be tracked accurately.

Proof 5: Consider the following Lyapunov function:

$$V_2 = \frac{1}{2} u_e^2 \tag{38}$$

Taking the time derivative of V_2, together with (37), yields

$$\begin{aligned}\dot{V}_2 =& u_e[\frac{1}{m_{11}}(m_{22} v r - d_{11} u + \tau_u + \tau_{\delta_u}) - \dot{u}_d] \\ =& u_e[\frac{1}{m_{11}}(\tau_{\delta_u} - \hat{\tau}_{\delta_u} - m_{11}(k_u u_e - \dot{u}_d)) - \dot{u}_d] \\ =& u_e[\frac{1}{m_{11}}(-m_{11}(k_u u_e - \dot{u}_d)) - \dot{u}_d] \\ =& -2k_u V_2\end{aligned} \tag{39}$$

where $2k_u > 0$, $\tau_{\delta_u} \equiv \hat{\tau}_{\delta_u}, \forall t \geq T_{obs}$ proven in (36), and the asymptotic stability is guaranteed

$$\lim_{t\to\infty} u_e = 0 \tag{40}$$

This concludes the proof.

This article has been accepted for publication in a future issue of this journal, but has not been fully edited. Content may change prior to final publication. Citation information: DOI 10.1109/ACCESS.2018.2797084, IEEE Access

B. HEADING CONTROL

Theorem 5: Consider yaw dynamics in (6), and an FDO-based robust heading tracking control law as follows:

$$\begin{aligned}\tau_r = &(m_{22}-m_{11})uv + d_{33}r - \hat{\tau}_{\delta_r} \\ &+ m_{33}(k_r(r-r_d)+\psi-\psi_d-\dot{r}_d)\end{aligned} \tag{41}$$

where $k_r > 0$, ψ_d is the guided heading angle in (21), and $\hat{\tau}_{\delta_r}$ is the estimate of external disturbances in yaw obtained in (33). r_d is a virtual signal given by

$$r_d = -k_\psi(\psi-\psi_d)+\dot{\psi}_d \tag{42}$$

where $k_\psi > 0$. Then, the desired heading angle ψ_d can be tracked accurately.

Proof 6: Consider the Lyapunov function as follows:

$$V_3 = \frac{1}{2}(\psi_e^2 + r_e^2) \tag{43}$$

where $\psi_e = \psi - \psi_d$, $r_e = r - r_d$ are the corresponding tracking errors.

Differentiating V_3 with respect to time, we obtain

$$\begin{aligned}\dot{V}_3 =&\psi_e(r-\dot{\psi}_d) + r_e(\dot{r}-\dot{r}_d) \\ =&\psi_e(r-r_d+r_d-\dot{\psi}_d) + r_e(\dot{r}-\dot{r}_d) \\ =&-k_\psi\psi_e^2 + r_e(\dot{r}-\dot{r}_d+\psi_e) \\ =&-k_\psi\psi_e^2 + r_e(\frac{1}{m_{33}}(-(m_{22}-m_{11})uv \\ &-d_{33}r+\tau_r+\tau_{\delta_r})-\dot{r}_d+\psi_e)\end{aligned} \tag{44}$$

Substituting the heading tracking control law in (41) into (44) yields

$$\begin{aligned}\dot{V}_3 =&-k_\psi\psi_e^2 + r_e(\tau_{\delta_r}-\hat{\tau}_{\delta_r}-k_r(r-r_d)) \\ =&-k_\psi\psi_e^2 - k_r r_e^2 \\ \le&-k_{V_3}V_3\end{aligned} \tag{45}$$

where $k_{V_3} = 2\min\{k_\psi, k_r\}$, $\tau_{\delta_u} \equiv \hat{\tau}_{\delta_u}, \forall t \ge T_{obs}$ proven in (36), and the asymptotic stability is guaranteed

$$\lim_{t\to\infty}(\psi_e, r_e) = 0 \tag{46}$$

This concludes the proof.

C. SWAY DYNAMICS

Consider the sway dynamics rewritten as follows:

$$m_{22}\dot{v} = -m_{11}ur - d_{22}v + \tau_{\delta_v} \tag{47}$$

Note that unknown dynamics τ_{δ_v} is actually bounded in practice, i.e., $|\tau_{\delta_v}| \le \bar{\tau}_{\delta_v}$. Moreover, from above analysis, surge and yaw velocities are made bounded, i.e., $|u| \le \bar{u}$ and $|v| \le \bar{v}$. In this context, we have

$$\dot{v} \le -\frac{d_{22}}{m_{22}}v + d_v \tag{48}$$

where d_{22} is actually positive for an USV, and $d_v = (m_{11}\bar{u}\bar{r} + \bar{\tau}_{\delta_v})/m_{22} < \infty$.

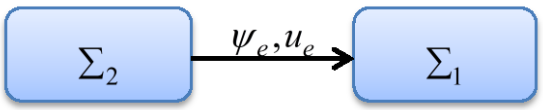

FIGURE 3. The modular of the cascade system.

Using Bellman-Gronwall comparison principle [50], we have

$$\begin{aligned}v(t) &\le v(t_0)e^{-\frac{d_{22}}{m_{22}}(t-t_0)} + \frac{d_v m_{22}}{d_{22}}\left(1-e^{-\frac{d_{22}}{m_{22}}(t-t_0)}\right) \\ &\le v(t_0) + \frac{d_v m_{22}}{d_{22}}, \quad \forall\, t_0 \le t < \infty\end{aligned} \tag{49}$$

In this context, sway velocity v is bounded by the surge, yaw dynamics and complex unknowns.

VIII. CLOSED-LOOP SYSTEM STABILITY ANALYSIS

As shown in Fig. 3, the path-following and tracking error dynamics can be formulated in a cascade form as follows:

$$\Sigma_1 : \begin{cases}\dot{x}_e = u_d\cos(\psi_d-\phi_p) + \dot{\phi}_p y_e - u_{\text{tar}} \\ \qquad -u_d\sin(\psi_d-\phi_p)\tan\beta_d + D_{x_e} \\ \dot{y}_e = u_d\sin(\psi_d-\phi_p) - \dot{\phi}_p x_e \\ \qquad +u_d\cos(\psi_d-\phi_p)\tan\beta_d + D_{y_e}\end{cases} \tag{50}$$

where

$$\begin{aligned}D_{x_e}(u_e,\psi_e,\beta_e) =&[u_e+(\cos\psi_e-1)u_d]\frac{\cos(\psi-\phi_p+\beta)}{\cos\beta} \\ &-\sin\psi_e u_d\frac{\sin(\psi-\phi_p+\beta)}{\cos\beta} \\ &-u_d\sin(\psi_d-\phi_p)\frac{\sin\beta_e}{\cos\beta\cos\beta_d} \\ D_{y_e}(u_e,\psi_e,\beta_e) =&[u_e+(\cos\psi_e-1)u_d]\frac{\sin(\psi-\phi_p+\beta)}{\cos\beta} \\ &-\sin\psi_e u_d\frac{\cos(\psi-\phi_p+\beta)}{\cos\beta} \\ &-u_d\cos(\psi_d-\phi_p)\frac{\sin\beta_e}{\cos\beta\cos\beta_d}\end{aligned} \tag{51}$$

which implies that

$$D_{x_e}(0) = D_{y_e}(0) = 0 \tag{52}$$

where $\beta_e = \beta - \hat{\beta}$, and $\beta_e \equiv 0, \forall t \ge T_{\text{obs}}$.

The surge and heading tracking error dynamics are reformulated as follows:

$$\Sigma_2 : \begin{cases}\dot{u}_e = \frac{1}{m_{11}}(m_{22}vr - d_{11}u + \tau_u + \tau_{\delta_u}) - \dot{u}_d \\ \dot{\psi}_e = r_d - \dot{\psi}_d + r_e \\ \dot{r}_e = \frac{1}{m_{33}}[-(m_{22}-m_{11})uv - d_{33}r \\ \qquad +\tau_r + \tau_{\delta_r}] - \dot{r}_d\end{cases} \tag{53}$$

Theorem 6: The finite-time observer based guidance and control (FOGC) scheme consisting of SLOS guidance law given by (21)–(23) together with the control laws (37) and

This article has been accepted for publication in a future issue of this journal, but has not been fully edited. Content may change prior to final publication. Citation information: DOI 10.1109/ACCESS.2018.2797084, IEEE Access

(41) render the entire guidance-control system (50) and (53) globally asymptotically stable.

Proof 7: From Theorems 4 and 5, we can directly find that Σ_2-subsystem (53) can be made globally asymptotically stable by virtual of control laws (37) and (41). In addition, by Theorem 2, Σ_1-subsystem (50) can be rendered globally asymptotically stable by using the SLOS guidance scheme (17), (21)–(23). Eventually, using Lemma 1, we can conclude that the entire closed-loop system (50) and (53) is globally asymptotically stable.

This concludes the proof.

IX. SIMULATION STUDIES

In order to demonstrate the effectiveness and superiority of the proposed FOGC scheme, simulation studies and comprehensive comparisons are conducted on the Cybership I [51], whereby the length is 1.19m, and the mass is 17.6kg. Inertia parameters are as follows: $m_{11} = 19\text{kg}$, $m_{22} = 35.2\text{kg}$, $m_{33} = 4.2\text{kg}$, $d_{11} = 4\text{kg/s}$, $d_{22} = 1\text{kg/s}$, $d_{33} = 10\text{kg/s}$.

Unknown external disturbances assumed as follows:

$$\boldsymbol{\tau}_\delta = 2\begin{bmatrix} \sin(0.5t + 0.3\pi) \\ \cos(0.5t + 0.1\pi) \\ \cos(0.5t + 0.2\pi) \end{bmatrix} \tag{54}$$

Initial kinematics and dynamics of the USV are as follows: $[x, y, \psi] = [10, 0, 0]$ and $[u, v, r] = [0, 0, 0]$.

The desired path is parameterized by:

$$\begin{cases} x_p(\varpi) = 10\sin(0.1\varpi) + \varpi \\ y_p(\varpi) = \varpi \end{cases} \tag{55}$$

where $\varpi(t)$ is governed by

$$\dot{\varpi} = \frac{u_{\text{tar}}}{\sqrt{x_p'^2(\varpi) + y_p'^2(\varpi)}} \tag{56}$$

where u_{tar} is defined by (23).

Moreover, surge and heading guidance signals are designed as follows:

$$\begin{cases} u_d = 2 + 0.2\sin(0.08\pi t) \\ \psi_d = \phi_p - \arctan(\tan\hat{\beta} + \frac{y_e}{\Delta}) \end{cases} \tag{57}$$

where the lookahead distance $\Delta = 1.2$.

The design parameters of the FOGC scheme are chosen as follows: $\lambda_1 = 0.1$, $\lambda_2 = 0.001$, $L_\beta = 1200$, $\lambda_3 = 0.2$, $\lambda_4 = 0.01$, $\boldsymbol{L}_\delta = \text{diag}(200, 200, 200)$, $k_1 = 1$, $k_u = 1$, $k_\psi = 1$, $k_r = 1$.

A. PERFORMANCE IMPROVEMENT WITH FSO

In this subsection, a comparison analysis that the sideslip angle is exactly estimated and compensated or not, is given to demonstrate the performance improvement with FSO. Actual and desired paths are shown in Fig. 4, from which we can see that the proposed FOGC scheme can achieve higher path-following accuracy than the finite-time disturbance observer based guidance-control (FDOGC) scheme without accurate sideslip angle compensation. The significant gaps of along-

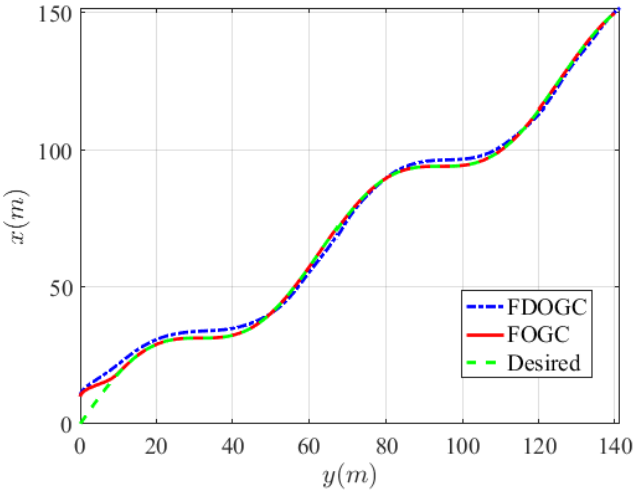

FIGURE 4. Path following performance.

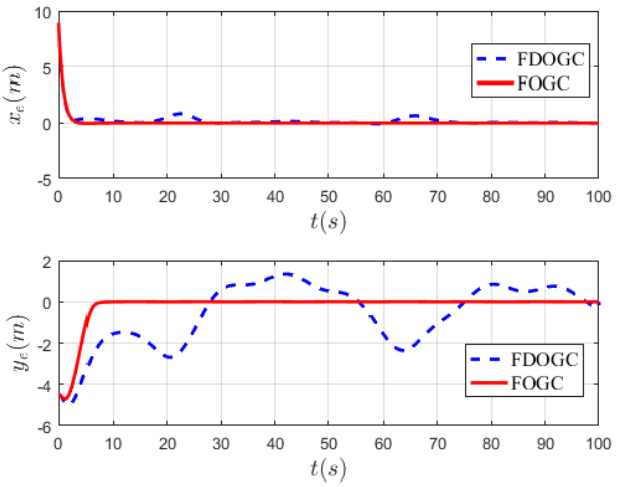

FIGURE 5. Cross- and along-track errors.

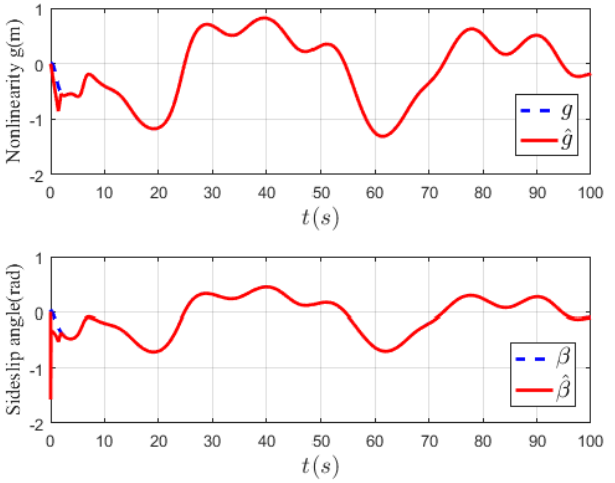

FIGURE 6. Estimates of unknown nonlinearity g and sideslip angle β.

This article has been accepted for publication in a future issue of this journal, but has not been fully edited. Content may change prior to final publication. Citation information: DOI 10.1109/ACCESS.2018.2797084, IEEE Access

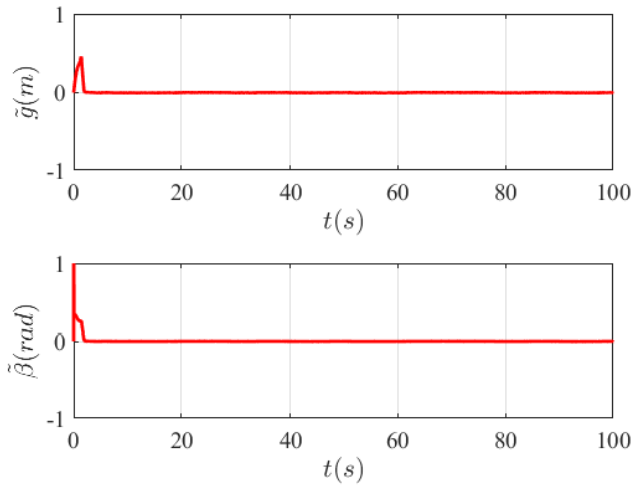

FIGURE 7. Estimate errors of unknown nonlinearity g and sideslip angle β.

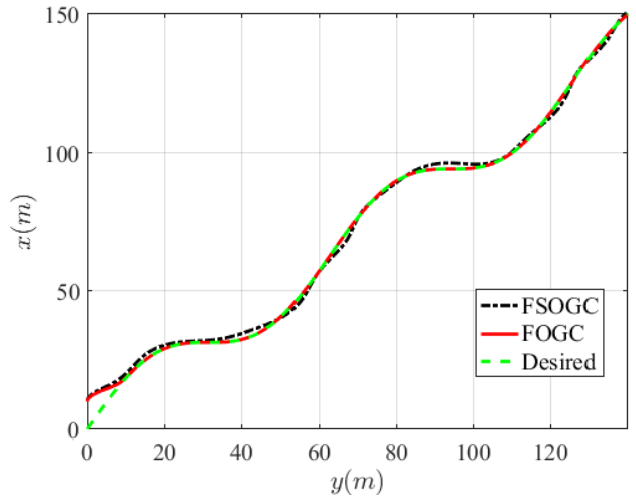

FIGURE 8. Path following performance.

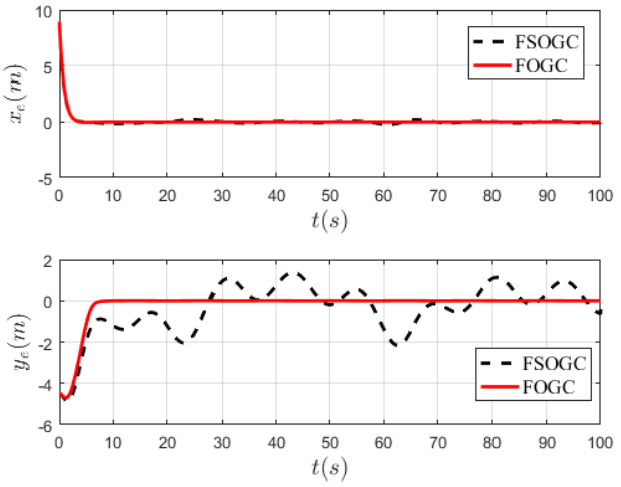

FIGURE 9. Cross- and along-track errors.

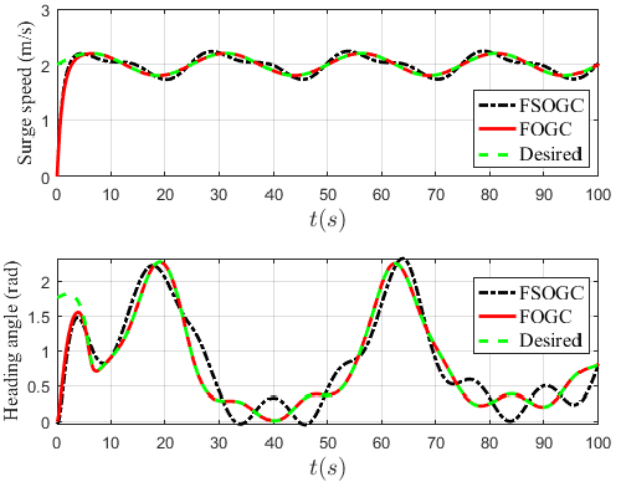

FIGURE 10. Surge speed and heading angle tracking.

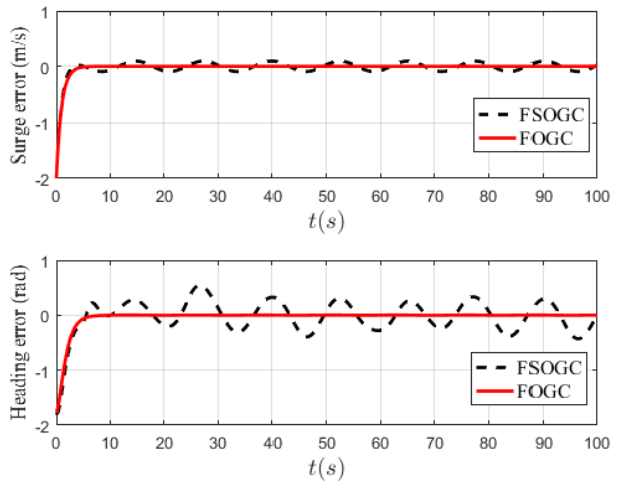

FIGURE 11. Surge and heading tracking errors.

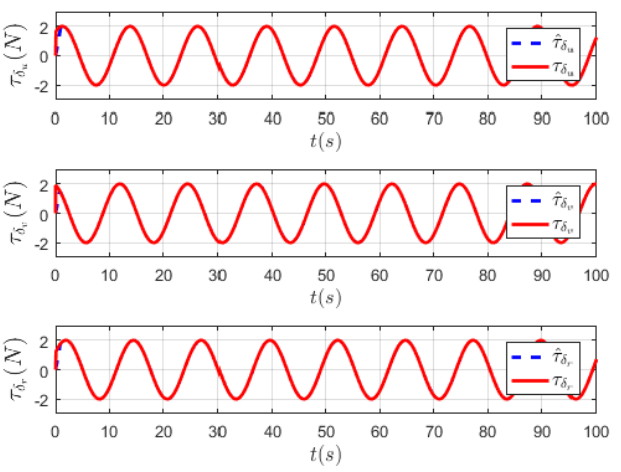

FIGURE 12. Estimates of external disturbances.

This article has been accepted for publication in a future issue of this journal, but has not been fully edited. Content may change prior to final publication. Citation information: DOI 10.1109/ACCESS.2018.2797084, IEEE Access

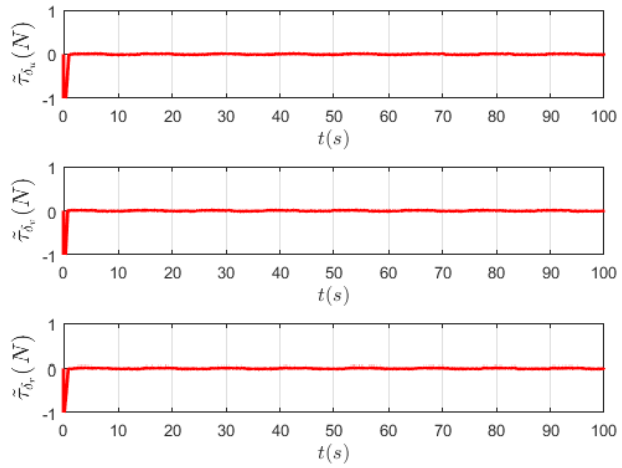

FIGURE 13. Disturbance estimate errors.

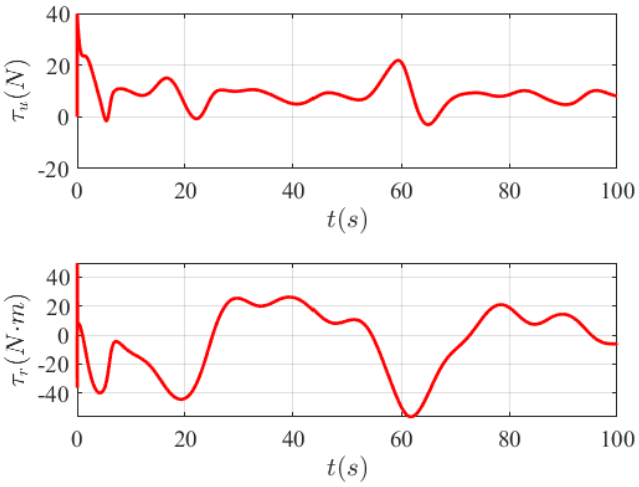

FIGURE 14. Control inputs.

and cross-track errors convergence are shown in Fig. 5, from which it can be observed that the FOGC scheme renders both along- and cross-track errors converge smoothly to zero within a short time. Form Figs. 6–7, one can see that the sideslip angle can be identified precisely. Therefore, we can conclude that the FSO can achieve accurate sideslip angle estimate and improve the path following accuracy.

B. PERFORMANCE IMPROVEMENT WITH FDO

In the subsection, the impact of external disturbances on the system is analyzed. Form Figs 8–9, we can see that, in comparison with the finite-time sideslip observer based guidance-control (FSOGC) scheme without the FDO, the proposed FOGC scheme can achieve higher path-following accuracy and stronger disturbance rejection, simultaneously. Figs. 10–11 show remarkable control effect of the proposed FOGC scheme in the presence of unknown external disturbances. In the contrast, without the constructed FDO, surge and heading tracking cannot be achieved accurately. Figs 12–13 show the precise unknown disturbance estimate. In this context, it can be concluded that remarkable performance and significant superiority of the proposed FOGC scheme is demonstrated. As shown in Fig. 14, the control force and moment are smooth and realistic from practical viewpoint.

In summary, the overall FOGC scheme can achieve exact path following together with accurate sideslip angle and disturbance observations in presence of time-varying large sideslip angle and unknown external disturbances.

X. CONCLUSIONS

In this paper, the problem of path following control for an USV, which suffers from time-varying large sideslip angle and unknown external disturbances, has been solved by devising an FOGC scheme. The time-varying large sideslip angle and unknown external disturbances have been exactly estimated by the FSO and the FDO, respectively, which render the estimate errors exactly converge to the origin within a short time. By virtue of the FSO, the proposed SLOS guidance guarantees complete sideslip angle feedback and avoids singularity in path-following process, such that both cross- and along-track errors are globally asymptotically stable. Combining backstepping technique with finite-time disturbance observation, FDO-based surge and heading robust tracking controllers have been created to render both surge and heading tracking errors globally asymptotically stable. Furthermore, the asymptotic stability of the entire guidance-control closed-loop system has been proven by cascade analysis. Eventually, the proposed FOGC scheme can achieve accurate path following of an USV suffering from unknown sideslip angle and disturbances.

ACKNOWLEDGMENT

The authors would like to thank the Editor-in-Chief, Associate Editor and anonymous referees for their invaluable comments and suggestions.

REFERENCES

[1] R. B. Wynn, V. A. I. Huvenne and T. P. L. Bas, "Autonomous underwater vehicles: Their past, present and future contributions to the advancement of marine geoscience," *Mar. Geol.*, vol. 352, no. 2, pp. 451–468, Jun. 2014.

[2] Y. Xu and K. Xiao, "Technology development of autonomous ocean vehicle," *Acta Auto. Sinica*, vol. 33, no. 5, pp. 518–521, May. 2007.

[3] N. Wang, M. J. Er and M. Han, "Large tanker motion model identification using generalized ellipsoidal basis functionbased fuzzy neural networks," *IEEE Trans. Cybern.*, vol. 45, no. 12, pp. 2732–2743, Jan. 2015.

[4] N. Wang, M. J. Er and M. Han, "Dynamic tanker steering control using generalized-ellipsoidal-basis-function-based fuzzy neural networks," *IEEE Trans. Fuzzy Syst.*, vol. 23, no. 5, pp. 1414–1427, Oct. 2015.

[5] M. Caccia, M. Bibuli, R. Bono and G. Bruzzone, "Basic navigation, guidance and control of an unmanned surface vehicle," *Auton. Robot.*, vol. 25, no. 4, pp. 349–365, Nov. 2008.

[6] D. Zhu, H. Huang and S. X. Yang, "Dynamic task assignment and path planning of multi-AUV system based on an improved self-organizing map and velocity synthesis method in threedimensional underwater workspace," *IEEE Trans. Cybern.*, vol. 43, no. 2, pp. 504–514, Mar. 2012.

[7] Y. Xia, G. Xu, K. Xu, Y. Chen, X. Xiang and Z. Ji, "Dynamics and control of underwater tension leg platform for diving and leveling," *Ocean Eng.*, vol. 109, pp. 454–478, Nov. 2015.

[8] N. Wang, C. J. Qian, J. C. Sun and Y. C. Liu, "Adaptive robust finite-time trajectory tracking control of fully actuated marine surface vehicles," *IEEE Trans. Control Syst. Technol.*, vol. 24, no. 4, pp. 1454–1462, Nov. 2016.

[9] A. M. Lekkas and T. I. Fossen, "Minimization of cross-track and along-track errors for path tracking of marine underactuated vehicles," In *Proc. Euro. Control Conf.*, Strasbourg, France, 2014, pp. 3004–3010.

[10] T. I. Fossen, "Guidance and Control of Ocean Vehicle," Wiley, New York, 1994.

[11] T. I. Fossen, M. Breivik and R. Skjetne, "Line-of-sight path following of underactuated marine craft," In *Proc. 6th IFAC Conf. Manoeuvr. Control Marine Craft.*, Trondheim, Norway, 2003, pp. 211–216.

[12] M. Breivik and T. I. Fossen, "Path following for marine surface vessels," In *Proc. MTTS/IEEE TECHNO-OCEAN'04*, Kobe, Japan, 2005, pp. 2282–2289.

[13] K. Y. Pettersen and E. Lefeber, "Waypoint tracking control of ships," In *Proc. IEEE Conf. Decision Control*, Orlando, FL, USA, 2001, pp. 940–945.

[14] T. I. Fossen and K. Y. Pettersen, "On uniform semiglobal exponential stability (USGES) of proportional line-of-sight guidance laws," *Automatica*, vol. 50, no. 11, pp. 2912–2917, Nov. 2014.

[15] E. Bϕrhaug, A. Pavlov and K. Y. Pettersen, "Integral LOS control for path following of underactuated marine surface vessels in the presence of constant ocean currents," In *Proc. IEEE Conf. Decision Control*, Cancun, Mexico, 2008, pp. 4984–4991.

[16] W. Caharija and K. Y. Pettersen, "Integral line-of-Sight guidance and control of underactuated marine vehicles: Theory, simulations, and experiments," *IEEE Trans. Control Syst. Technol.*, vol. 24, no. 5, pp. 1623–1642, Feb. 2016.

[17] A. M. Lekkas and T. I. Fossen, "Integral LOS path following for curved paths based on a monotone cubic hermite spline parametrization," *IEEE Trans. Control Syst. Technol.*, vol. 22, no. 6, pp. 2287–2301, Mar. 2014.

[18] T. I. Fossen, K. Y. Pettersen and R. Galeazzi, "Line-of-sight path following for dubins paths with adaptive sideslip compensation of drift forces," *IEEE Trans. Control Syst. Technol.*, vol. 23, no. 2, pp. 820–827, Jul. 2015.

[19] T. I. Fossen and A. M. Lekkas, "Direct and indirect adaptive integral line-of-sight path following controllers for marine craft exposed to ocean current," *Int. J. Adapt. Control*, vol. 31, no. 4, pp. 445–463, Mar. 2017.

[20] J. Miao, S. Wang, Z. Zhao, Y. Li and M. M. Tomovic, "Spatial curvilinear path following control of underactuated AUV with multiple uncertainties," *ISA Trans.*, vol. 67, pp. 107–130, Mar. 2017.

[21] S. R. Oh and J. Sun, "Path following of underactuated marine surface vessels using line-of-sight based model predictive control," *Ocean Eng.*, vol. 37, no. 2, pp. 289–295, Feb. 2010.

[22] Z. Yan, H. Yu, W. Zhang, B. Li and J. Zhou, "Globally finite-time stable tracking control of underactuated UUVs," *Ocean Eng.*, vol. 107, pp. 132–146, Aug. 2015.

[23] B. Yi, L. Qiao and W. Zhang, "Two-time scale path following of underactuated marine surface vessels: Design and stability analysis using singular perturbation methods," *Ocean Eng.*, vol. 124, pp. 287–297, Sep. 2016.

[24] J. H. Li, P. M. Lee and B. H. Jun, "Point-to-point navigation of underactuated ships," *Automatica*, vol. 44, no. 12, pp. 3201–3205, Dec. 2008.

[25] Q. Zou, F. Wang, L. Zou and Q. Zong, "Robust adaptive constrained backstepping flight controller design for re-entry reusable launch vehicle under input constraint," *Adv. Mech. Eng.*, vol. 7, no. 9, pp. 1–13, Sep. 2015.

[26] X. Xiang, C. Liu, H. Su and Q. Zhang, "On decentralized adaptive full-order sliding mode control of multiple UAVs," *ISA Trans.*, 2017, DOI:10.1016/j.isatra.2017.09.008

[27] K. Shojaei and M. Dolatshahi, "Line-of-sight target tracking control of underactuated autonomous underwater vehicles," *Ocean Eng.*, vol. 133, pp. 224–252, Mar. 2017.

[28] J. Xu, M. Wang and G. Zhang, "Trajectory tracking control of an underactuated unmanned underwater vehicle synchronously following mother submarine without velocity measurement," *Adv. Mech. Eng.*, vol. 7, no. 7, pp. 1–11, Jul. 2015.

[29] D. Niu, X. Chen, J. Yang, X. Wang and X. Zhou, "Composite control for raymond mill based on model predictive control and disturbance observer," *Adv. Mech. Eng.*, vol. 8, no. 3, pp. 1–11, Mar. 2016.

[30] N. Wang, J. C. Sun, M. Han, Z. Zheng and M. J. Er, "Adaptive approximation-based regulation control for a class of uncertain nonlinear systems without feedback linearizability," *IEEE Trans. Neural Netw. Learn. Syst.*, 2017, DOI: 10.1109/TNNLS.2017.2738918

[31] N. Wang and M. J. Er, "Direct adaptive fuzzy tracking control of marine vehicles with fully unknown parametric dynamics and uncertainties," *IEEE Trans. Control Syst. Technol.*, vol. 24, no. 5, pp. 1845–1852, Sep. 2016.

[32] N. Wang, J. C. Sun and M. J. Er, "Tracking-error-based universal adaptive fuzzy control for output tracking of nonlinear systems with completely unknown dynamics," *IEEE Trans. Fuzzy Syst.*, 2017, DOI: 10.1109/TFUZZ.2017.2697399

[33] N. Wang, J. C. Sun, M. J. Er and Y. C. Liu, "A novel extreme learning control framework of unmanned surface vehicles," *IEEE Trans. Cybern.*, vol. 46, no. 5, pp. 1106–1117, May. 2016.

[34] X. Xiang, C. Yu, L. Lapierre, J. Zhang and Q. Zhang, "Survey on fuzzy-logic-based guidance and control of marine surface vehicles and underwater vehicles," *Int. J. Fuzzy Syst.*, 2017, DOI:10.1007/s40815-017-0401-3

[35] N. Wang, Y. Gao, Z. Sun and Z. Zheng, "Nussbaum-based adaptive fuzzy tracking control of unmanned surface vehicles with fully unknown dynamics and complex input nonlinearities," *Int. J. Fuzzy Syst.*, 2017, DOI: 10.1007/s40815-017-0387-x

[36] N. Wang, M. J. Er, J. C. Sun and Y. C. Liu, "Adaptive robust online constructive fuzzy control of a complex surface vehicle system," *IEEE Transactions on Cybernetics*, vol. 46, no. 7, pp. 1511–1523, Jul. 2016.

[37] N. Wang and M. J. Er, "Self-constructing adaptive robust fuzzy neural tracking control of surface vehicles with uncertainties and unknown disturbances," *IEEE Trans. Control Syst. Technol.*, vol. 23, no. 3, pp. 991-1002, May. 2015.

[38] N. Wang, S. F. Su, J. Yin, Z. Zheng and M. J. Er, "Global asymptotic model-free trajectory-independent tracking control of an uncertain marine vehicle: An adaptive universe-based fuzzy control approach," *IEEE Trans. Fuzzy Syst.*, 2017, DOI: 10.1109/TFUZZ.2017.2737405

[39] J. Miao, S. Wang, Z. Zhao, Y. Li and M. M. Tomovic, "Spatial curvilinear path following control of underactuated AUV with multiple uncertainties," *ISA Trans.*, vol. 67, pp. 107–130, Mar. 2017.

[40] S. Liu, Y. C. Liu and N. Wang, "Nonlinear disturbance observerbased backstepping finite-time sliding mode tracking control of underwater vehicles with system uncertainties and external disturbances," *Nonlinear Dynam.*, vol. 88, no. 1, pp. 465–476, Dec. 2017.

[41] N. Wang, C. J. Qian and Z. Y. Sun, "Global asymptotic output tracking of nonlinear second-order systems with power integrators," *Automatica*, vol. 80, pp. 156-161, Jun. 2017.

[42] Y. Feng, X. H. Xu and Z. H. Man, "Non-singular terminal sliding mode control of rigid manipulators," *Automatica*, vol. 38, no. 12, pp. 2159–2167, Dec. 2002.

[43] N. Wang, S. Lv, M. J. Er and W. H. Chen, "Fast and accurate trajectory tracking control of an autonomous surface vehicle with unmodelled dynamics and disturbances," *IEEE Trans. Intell. Veh*, vol. 1, no. 3, pp. 230–243, Jan. 2016.

[44] N. Wang, S. Lv, W. Zhang, Z. Liu and M. J. Er, "Finite-time observer based accurate tracking control of a marine vehicle with complex unknowns," *Ocean Eng.*, vol. 145, pp. 406–415, Nov. 2017.

[45] N. Wang, Z. Sun, Z. Zheng and H. Zhao, "Finite-time sideslip observer-based adaptive fuzzy path-following control of underactuated marine vehicles with time-varying large sideslip," *Int. J. Fuzzy Syst.*, 2017, DOI: 10.1007/s40815-017-0392-0

[46] V. Sundarapandian, "Global asymptotic stability of nonlinear cascade systems," *Appl. Math. Lett.*, vol. 15, no. 3, pp. 275–277, Apr. 2002.

[47] Y. B. Shtessel, I. A. Shkolnikov and A. Levant, "Smooth second-order sliding modes: Missile guidance application," *Automatica*, vol. 43, no. 8, pp. 1470–1476, Aug. 2007.

[48] T. I. Fossen, "Handbook of Marine Craft Hydrodynamics and Motion Control," John Wiley & Sons Ltd, New York, 2011.

[49] X. Xiang, L. Lapierre and B. Jouvencel, "Smooth transition of AUV motion control: From fully-actuated to under-actuated configuration," *Robot. Auton. Syst.*, vol. 67, pp. 14–22, Oct. 2015.

[50] H. Khalil, "Nonlinear Systems," 3nd ed. Prentice-Hall Press, Upper Saddle River, NJ, USA, 2002.

[51] J. Ghommam, F. Mnif, A. Benali and G. Poisson, "Observer design for euler lagrange systems: Application to path following control of an underactuated surface vessel," In *Proc. IEEE/RSJ Inter. Conf. Intell. Robot. Syst.*, San Diego, CA, USA, 2007, pp. 2883–2888.

This article has been accepted for publication in a future issue of this journal, but has not been fully edited. Content may change prior to final publication. Citation information: DOI 10.1109/ACCESS.2018.2797084, IEEE Access

NING WANG (S'08-M'12-SM'15) received the B. Eng. degree in marine engineering and the Ph.D. degree in control theory and engineering from the Dalian Maritime University (DMU), Dalian, China, in 2004 and 2009, respectively. From 2008 to 2009, he was a joint-training Ph.D. student with Nanyang Technological University, Singapore, financially supported by China Scholarship Council. From 2014 to 2015, he was a Visiting Scholar with The University of Texas at San Antonio, San Antonio. He is currently a Full Professor with the Marine Engineering College, DMU.

Dr. Wang research interests include fuzzy neural systems, deep learning, nonlinear control, self-organizing fuzzy neural modeling and control, unmanned vehicles and autonomous control. He received the Nomination Award of Liaoning Province Excellent Doctoral Dissertation, the DMU Excellent Doctoral Dissertation Award, the DMU Outstanding Ph.D. Student Award in 2010, the Excellent Government-funded Scholars and Students Award in 2009 from NTU. He was a recipient of the Liaoning Province Award for Technological Invention and the honor of Liaoning BaiQianWan Talents, Liaoning Excellent Talents, Science and Technology Talents the Ministry of Transport of the P. R. China, Youth Science and Technology Award of China Institute of Navigation, and Dalian Leading Talents. He currently serves as an Associate Editor of the *Neurocomputing* and the *International Journal of Fuzzy Systems*, and a Leading Guest Editor of the *Advances in Mechanical Engineering.*

ZHUO SUN received his B. Eng. degree in Marine Electronic and Electrical Engineering from the Dalian Maritime University (DMU), Dalian, China in 2016. He is currently pursuing his Master degree at DMU, Dalian 116026. His research interests include underactuated marine vehicle, fuzzy modeling and control, and finite-time control.

JIANCHUAN YIN (M'10) received his Ph.D. degree in traffic information engineering from Dalian Maritime University (DMU), Dalian, China in 2007. He is an associate professor with the Navigation College, DMU, Dalian 116026, China. He is currently a visiting scholar with Department of Naval Architecture and Marine Engineering, University of Michigan, Ann Arbor, Michigan 48109, USA. His research interests include computational intelligence and ocean engineering.

SHUN-FENG SU (F'10) received the B.S. degree in electrical engineering from National Taiwan University, Taipei, Taiwan, in 1983 and the M.S. and Ph.D. degrees in electrical engineering from Purdue University, West Lafayette, IN, USA, in 1989 and 1991, respectively.

He is currently a Chair Professor with the Department of Electrical Engineering, National Taiwan University of Science and Technology, Taipei. He has published more than 160 refereed journal and conference papers in the areas of robotics, intelligent control, fuzzy systems, neural networks, and nonderivative optimization. His current research interests include computational intelligence, machine learning, virtual reality simulation, intelligent transportation systems, smart home, robotics, and intelligent control.

Dr. Su is a Chinese Automatic Control Society (CACS) Fellow. He is the President of the Taiwan Fuzzy System Association and a Vice President of the International Fuzzy Systems Association. He currently serves on the Board of Governors of the CACS, the Taiwan Society of Robotics, and the Taiwan Association of System Science and Engineering. He is currently an Associate Editor for the *IEEE Transactions on Cybernetics* and the *IEEE Transactions on Systems*, as well as an Area Editor of the *International Journal of Fuzzy Systems*.

SANJAY SHARMA received the B.Tech. (Hons.) degree in electrical engineering from the Indian Institute of Technology Kharagpur, Kharagpur, India, the M.Tech. (Hons.) degree in control systems from the Indian Institute of Technology (BHU) Varanasi, Varanasi, India, and the Ph.D. degree in control and systems engineering from the University of Sheffield, Sheffield, U.K.

He is a Reader with the School of Marine Science and Engineering, University of Plymouth, Plymouth, U.K., and the Head of the Autonomous Marine Systems Research Group. He is a member of the IMechEs Marine, Informatics and Control Group and also the IFAC Technical Committee on Intelligent Autonomous Vehicles. He has authored over 70 book, journal, and refereed conference publications. His current research interests include design, development and application of artificial intelligence techniques and evolutionary algorithms in navigation, guidance, and control of marine robotics and unmanned marine craft.